**Linking HYSYS with CFD: Study of Centrifugal Compressor Operations**

by

Muhammad Zakwan bin Mohd Sahak

Dissertation submitted in partial fulfilment of

the requirements for the

Bachelor of Engineering (Hons)

(Chemical Engineering)

SEPTEMBER 2011

Universiti Teknologi PETRONAS

Bandar Seri Iskandar,

31750 Tronoh,

Perak Darul Ridzuan.

# CERTIFICATION OF APPROVAL

**Linking CFD with HYSYS: Study of Centrifugal Compressor Operation**

by

Muhammad Zakwan bin Mohd Sahak

A project dissertation submitted to the
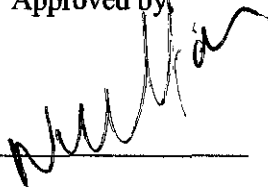
Chemical Engineering Programme

Universiti Teknologi PETRONAS

in partial fulfillment of the requirement for the

BACHELOR OF ENGINEERING (Hons)

(CHEMICAL ENGINEERING)

Approved by

_____

(AP Dr Nurul Hasan)

UNIVERSITI TEKNOLOGI PETRONAS

TRONOH, PERAK

SEPTEMBER 2011

ii

# CERTIFICATION OF ORIGINALITY

This is to certify that I am responsible for the work submitted in this project, that the original work is my own except as specified in the references and acknowledgements, and that the original work contained herein have not been undertaken or done by unspecified sources or persons.

MUHAMMAD ZAKWAN BIN MOHD SAHAK

# ABSTRACT

The flow through a centrifugal compressor which consists of 20 impeller blades and 19 diffuser blades is simulated using NUMECA FINE/Turbo. The geometry of the compressor was done by using AutoBlade. Test variations were conducted for meshing and discretization for selecting the best alternative for the test. The result is validated using a published journal. The values and parameters of the simulation result were then transferred to Aspen HYSYS to see the agreement of the values. An error of 0.19% is obtained from the static temperature at outlet.

# ACKNOWLEDGEMENT

In the name of Allah S.W.T, The Most Gracious, The Most Merciful, all praises to Him for His gratitude, blessings and opportunity. The author would like to acknowledge the following parties for their help and support during the completion of the final year project:

    i)  Department of Chemical Engineering, UTP.
    ii)  NUMIT Enterprise Sdn. Bhd.

A special acknowledgement and gratitude to AP Dr Nurul Hasan, the Director of Advanced Simulation Lab, who was the author's supervisor, for his involvement and kind support towards the author in completing the project.

The author would also like to expose his gratitude to his family, friends and others who were involved, directly and indirectly, in ensuring the successfulness of the final year project. Their help and support are highly appreciated.

Thank you very much.

# TABLE OF CONTENTS

# LIST OF TABLES

# LIST OF FIGURES

# ABBREVIATIONS AND NOMENCLATURES

$\delta$ – boundary layer thickness

$\delta_v^*$ – displacement thickness

$\nu_t$ – eddy viscosity

$l_{mix}$ – mixing length

$\omega$ – dissipation per unit turbulent kinetic energy (specific dissipation)

$y$ – vertical distance

$\kappa$ – von-Karman constant

$\rho$ – density

$y^+$ – dimensionless vertical distance (wall variables)

$F_{Kleb}$ – Klebanoff's intermittency function

$U_{dif}$ – maximum value of the velocity for boundary layers

$y_{max}$ – value of y at which $l_{mix}$ of $\omega$ achieves its maximum value

$d_i$ – inlet diameter

$d_o$ – outlet diameter

$h_i$ – inlet span

$h_o$ – outlet axial span

$\alpha_i$ – inlet blade angle

$\alpha_o$ – outlet blade angle

$n$ – number of blades

$V_z$ – axial velocity

M1 - initial mesh size

M2 - two times initial mesh size

M3 – three times initial mesh size

M4 – four times initial mesh size

CEN – $2^{nd}$ order central discretization

UPW1 – $1^{st}$ order upwind discretization

TVD – $2^{nd}$ order upwind discretization with symmetric TVD scheme

FLUX – $2^{nd}$ order upwind discretization with flux difference splitting scheme

BL – Baldwin-Lomax turbulence model

# CHAPTER 1:

# INTRODUCTION

## 1.1    Background of Study

Nowadays, the usage of process simulation software, such as Aspen HYSYS, is very wide in design process, which is very useful in giving an overview of how the real process will perform.

For further detailed design and analysis, computational fluid dynamics (CFD) can be used to model the characteristics of flow inside the unit operation. CFD will give a better view in term of interaction between particles, or in the micro level of the analysis. With the advancing technology, much CFD software is available in the market to assist with the analysis.

Given a unit operation, such as a centrifugal compressor, process simulators can be used to predict the value of parameters at its inlet and outlet, which is calculated according to the specified thermodynamic package. However, the process inside the compressor itself cannot be viewed by the process simulation software alone.

## 1.2    Problem Statement

Currently, there is no available technique that can relate the parameters from process simulators such as HYSYS with CFD software to give simultaneous result on the macro and micro level of process inside a unit operation i.e. centrifugal compressor.

If such relation exists, we can get the value of inlet and outlet parameters of the compressor, as well as the changes or process that is happening to the flow inside the compressor as well. The velocity distribution for example, can be predicted for the given inlet and outlet parameters value.

The reliability of value provided by HYSYS can also be studied with respect to the real operation, as CFD application gives a better prediction for a real process due to its ability to model on a micro level basis.

## 1.3 Objectives

This research project focuses on the following objectives:

1. To develop a working geometry of a centrifugal compressor.
2. To run a test for determining the best alternative in modeling the compressor operation.
3. To validate the result of the simulation with published journal data.
4. To seek the agreement of values or parameters between CFD and HYSYS.

# CHAPTER 2:

# LITERATURE REVIEW

## 2.1 Turbomachinery

Turbomachines, being one of the divisions of fluid machines, can be defined as devices that feature the continuous flow of a fluid through one or more rotating blade rows, and energy, as work, is extracted from or transferred to the fluid by the dynamic action of the blade rows (Logan, Kadambi, & Roy, 2003). In other words, turbomachines are energy conversion devices that convert mechanical energy to thermal/pressure energy or vice versa.

Turbomachines can be classified based on three categories (Peng, 2008):

a) Direction of energy transfer, either from mechanical to thermal/pressure or vice versa;

b) Type of fluid medium handled, either compressible or incompressible; and

c) Direction of flow through the rotating impeller, it can be axial, radial or mixed with respect to the rotational axis.

**Table 1** summarizes the classification of turbomachines.

**Table 1:** Classification of turbomachines

| Turbomachines | | |
|---|---|---|
| **Direction of energy transfer** | Pumping devices | Turbines |
| **Type of fluid (liquid/gas)** | Pump, fan, blower, compressor | Hydraulic, wind, gas, steam turbines |
| **Flow direction** | Axial-flow, mixed-flow, radial-flow | |
| **Mechanical arrangement** | Horizontal- or vertical-axis pump, single- or double-suction pump/fan, single- or multi-stage pump/compressor, backward-, radial- or forward-vane fan, full- or partial-admission turbine, horizontal- or vertical-axis wind turbine | |

## 2.2 Study of Centrifugal Compressor Operations

Compressors, a type of turbomachines, can also be defined as steady-flow engineering devices i.e. devices that operate essentially under the same conditions for a long period of time (Cengel & Boles, 2006). Compressor is driven by external work through a rotating shaft, usually turbine or motor, and is used to increase the pressure of fluid passing through it. **Figure 1** shows the schematics of a centrifugal compressor, a type of radial-flow compressor.



Arrows show direction of air flow
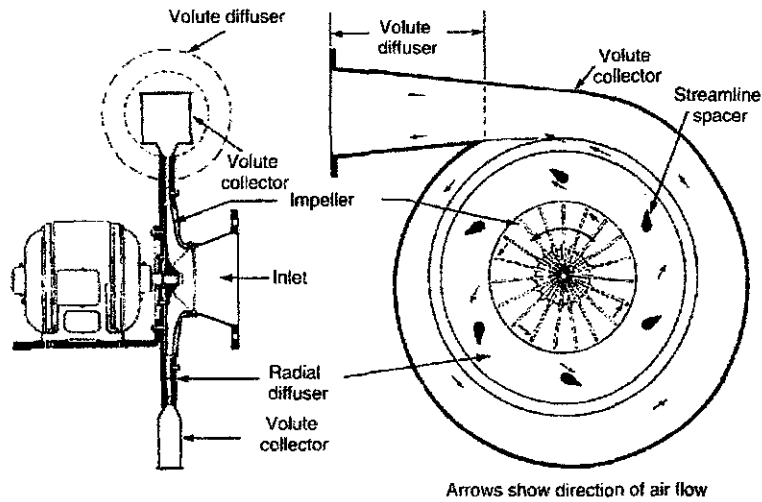
**Figure 1:** Schematics of centrifugal compressor **(Peng, 2008).**

Numerous studies had been carried out to investigate the distribution of velocity and pressure distribution inside a centrifugal compressor. Ubaldi et al. (1997) focused on experimental analysis to study the characteristics of flow inside the impeller of a centrifugal compressor using four beam two-color fibre optic laser-Doppler velocimeter. The sample of result is as shown in **Figure 2.**

Dickmann et al. (2006) in their study of three-dimensional computational fluid dynamics simulation and numerical and experimental analysis of impeller blade vibration, had conclude the possibilities of simulating unsteady flows through complex centrifugal compressor geometries for off-design conditions, attaining a calculated volume flow and pressure ratio over the entire stage nearly equal to the measured values. **Figure 3** shows the snapshot of the absolute velocities distribution inside the system.

5
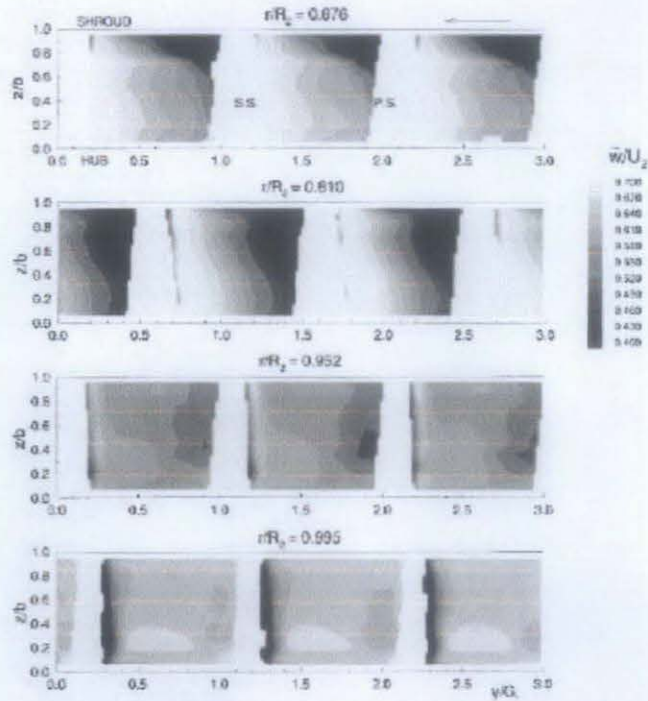
**Figure 2:** Ensemble-averaged relative velocity within the impeller (Ubaldi, Zunino, & Giglione, 1997).
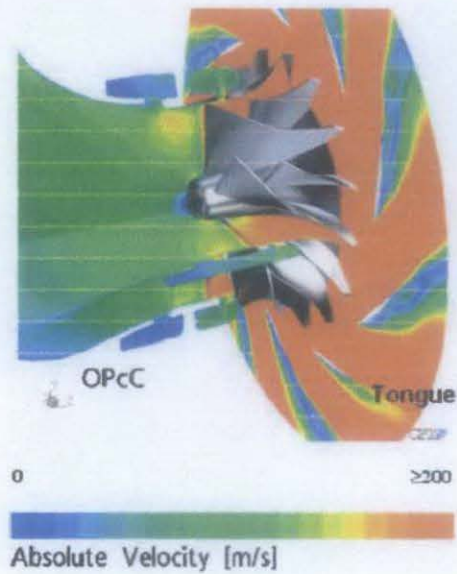


**Figure 3:** Snapshot of absolute velocities inside the centrifugal system (Dickmann, Wimmell, Szwedowicz, Filsinger, & Roduner, 2006).

Zhou et al. (2007) had compared the unsteady flow inside a centrifugal compressor using time-inclined operator and CFD simulation software. They managed to predict the velocity and pressure distribution inside a centrifugal compressor almost precisely with the actual data. **Figure 4** shows the result of the analysis.
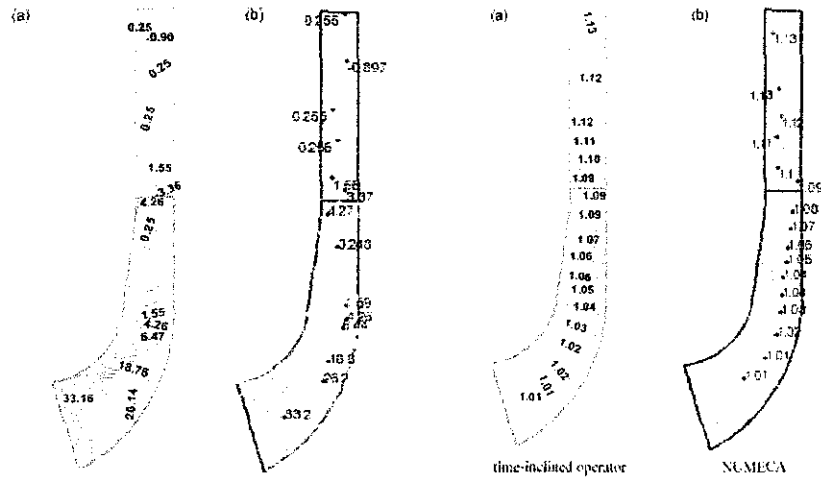


**Figure 4**: Comparison of axial velocity (left) and pressure (right) distribution between time-inclined operator and NUMECA (Zhou, Xi, & Cai, 2007).

Marconcini et al. (2008) had used a 3-D Navier Stokes solver to study the velocity distribution inside a transonic centrifugal compressor, and the result is compared with the detailed laser Doppler velocimetry flow measurements. **Figure 5** shows the meridional section of the impeller, and the sample of resulting flow measurement is shown in **Figure 6**.

7
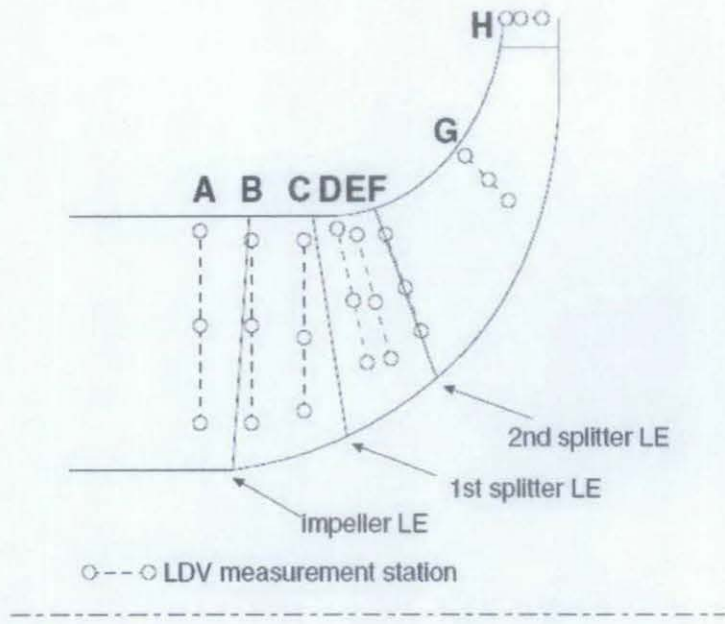
**Figure 5:** Meridional section of the impeller with measurement sections (Marconcini, Rubechini, & Ibaraki, 2008).
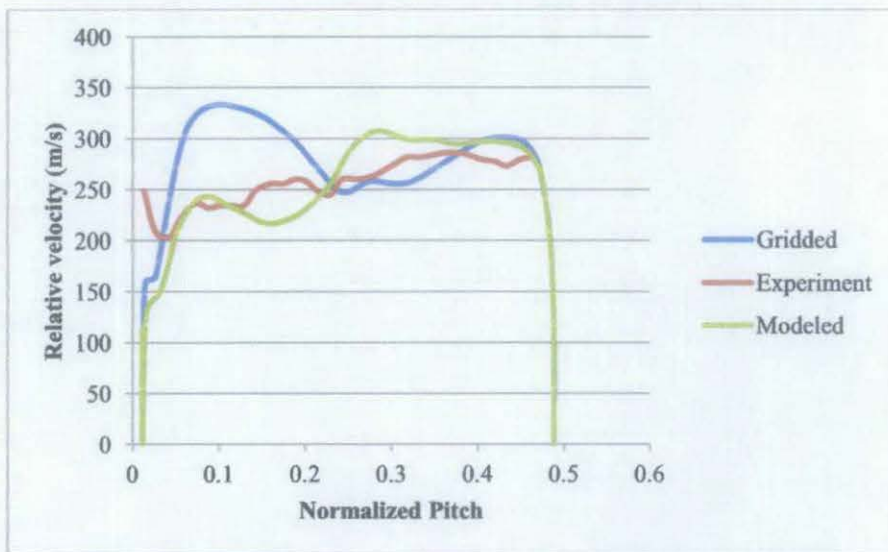


**Figure 6:** Relative velocity distribution for the shroud of section D (85-90% of blade span) (Marconcini, Rubechini, & Ibaraki, 2008).

## 2.3 Aspen HYSYS

Aspen HYSYS (or HYSYS) is one of the major process simulators, developed by AspenTech, which is widely used in chemical industries today. HYSYS will predict the result of the process simulation based on thermodynamic package chosen when running the simulation, usually in steady-state condition.

HYSYS is used in numerous researches to simulate a process or a plant in steady-state condition such as HEN-integrated natural gas turbo-expander plant (Konukman & Akman, 2005), $CO_2$ capture and compression unit (Zanganeh, Shafeen, & Salvador, 2009) and refrigeration cycles in ethylene and propylene production process (Fabrega, Rossi, & d'Angelo, 2010).

In this project, HYSYS will be used to model and simulate the turbine/compressor operation on a macro level.

## 2.4 Computaional Fluid Dynamics (CFD) and NUMECA Fine/Turbo™

Computational fluid dynamics (CFD) is one of the branches in fluid dynamics that uses numerical methods and algorithms to solve and analyze the problems that involve fluid flows.

With advancing computer technology, today's commercially available CFD software can be economically applied to turbomachine design and analysis. The main function of the CFD software is to develop a comprehensive numerical system to simulate the three-dimensional fluid flow at various parts of a machine.

The core part of CFD software is the numerical calculation scheme. The complete Navier-Stokes equations of different forms for three-dimensional compressible viscous fluid are converted into algebraic equations through the finite-element, finite-difference or control volume scheme. A numerical technique is then used to solve the simultaneous algebraic equations with respect to the boundary conditions. The postprocessor is used to manipulate the calculated result into convenient formats, either graphical or numerical.

NUMECA Fine/Turbo™, a type of CFD software, is widely used for problems mainly involving turbomachinery equipments such as steady numerical studies of the 3-D blade passage (Becker, Reyer, & Swoboda, 2007), numerical modeling of pressure drop of inclined flow through a heat exchanger for aero-engine applications (Missirlis, Yakinthos, Storm, & Goulas, 2007) and simulation for multi-block structured grids on the turbomachinery blades simulation (Derakhshan, Mohammadi, & Nourbakhsh, 2008).

NUMECA will be used to model the flowing fluid characteristics inside the centrifugal compressor.

## 2.5    Baldwin-Lomax Turbulence Model (1978)

The Baldwin-Lomax turbulence model is an algebraic or zero-equation model, which is one of the simplest turbulence models. It is used for applications where the boundary layer thickness, $\delta$, and displacement thickness, $\delta_v^*$, are not easily determined.

The model uses an inner and an outer layer eddy viscosity. The inner viscosity is given by

$$\nu_t = \left(l_{mix}\right)^2 |\omega| \quad y \le y_m \tag{1}$$

where the symbol, $\omega$, is the magnitude of the vorticity vector for three dimensional flows. The mixing length is calculated from the Van-Driest equation

$$l_{mix} = \kappa y \left[ 1 - \exp\left( -y^+ \Big/ A_0^+ \right) \right] \tag{2}$$

The outer viscosity is given by

$$\nu_t = \rho \alpha C_{cp} F_{Wake} F_{Kleb} \left( y, y_{max} \Big/ C_{Kleb} \right) \quad y > y_m \tag{3}$$

where

$$F_{Wake} = \min\left[ y_{max} F_{max}, \; C_{wk} y_{max} U_{dif}^2 \Big/ F_{max} \right] \tag{4}$$

$$F_{max} = \frac{1}{\kappa} \left[ \max_{y} \left( l_{mix} |\omega| \right) \right] \tag{5}$$

This model avoids the need to locate the boundary layer edge by calculating the outer layer length scale, in term of the vorticity, instead of the displacement or thickness.

11

$$\text{if } F_{Wake} = y_{max}F_{max} \quad \text{then } \delta_{r}^* = \frac{y_{mxz}^2 \omega}{U_c} \tag{6}$$

$$\text{if } F_{Wake} = \left. C_{wk}y_{max}U_{dif}^2 \middle/ F_{max} \right. \quad \text{then } \delta_{r}^* = \frac{U_{dif}}{|\omega|} \tag{7}$$

$y_{max}$ is the value of y at which $l_{mix}$ of $\omega$ achieves its maximum value, and $U_{dif}$ is the maximum velocity for boundary layers. The constants in this model are

$$\kappa = 0.40 \quad \alpha = 0.0168 \quad A_0^+ = 26$$
$$C_{cp} = 1.6 \quad C_{Kleb=0.3} \quad C_{wk} = 1$$

In general, the model performs reasonably well for free shear flows, but the mixing length specification for these flows is highly problem dependent. It gives good engineering predictions when compared to experimental values of the friction coefficients and velocity profiles, for wall bounded and boundary layer flows. Despite not reliable for predicting extraordinarily complex flows or separated flows, it has historically provided sound engineering solutions for problems within its range of applicability (Celik, 1999)

# CHAPTER 3:

# PROJECT WORK

## 3.1 Methodology

A published journal, Zhou et al. (2007), has been identified as the main reference, which the results will be reproduced using NUMECA and compared with the original results. Then, the resulting parameters will be transferred to HYSYS to obtain the between the results from both NUMECA and HYSYS.

Two types of test variation will be conducted; meshing and discretization. For meshing, the second and third test variation will be two and three times the number of mesh of the initial. Discretization will be based on central second order, and upwind, both first and second order. As for the turbulence model, Baldwin-Lomax is chosen following the journal selected (Zhou, Xi, & Cai, 2007).

The result of all test variations was analysed before being compared with the original results. After comparison of results was done, the parameters from NUMECA were fitted in HYSYS and the agreement between the values from both softwares is to be observed.

**Table 2** summarizes the test variations.

**Table 2:** Summary of test variations for the published journal.

| | 1st test | 2nd test variation | 3rd test variation | 4th test variation |
|---|---|---|---|---|
| **Meshing** | M1_CEN_BL | M2_CEN_BL | M3_CEN_BL | M4_CEN_BL |
| **Discretization** | MB_CEN_BL | MB_UPW1_BL | MB_TVD_BL | MB_FLUX_BL |

M1 is for initial mesh size, M2 is for 2 times initial mesh size, M3 is for 3 times initial mesh size, M4 is for 4 times initial mesh size, MB is for the best mesh from mesh test variations.

CEN is for 2nd order central discretization, UPW1 is for 1st order upwind discretization, TVD is for 2nd order upwind discretization with symmetric TVD scheme, FLUX is for 2nd order upwind discretization with flux difference splitting scheme.

BL is for Baldwin-Lomax turbulence model.

## 3.2 Geometry of the Compressor

Based on geometry data provided by Zhou et al. (2007), a standard middle stage of a centrifugal compressor is used to investigate the unsteady interaction flow between the impeller and vaned diffuser, which consists of a typical modern three-dimensional centrifugal impeller and an aerofoil diffuser. The geometry data is provided in **Table 3**.

**Table 3:** Geometrical data (Zhou, Xi et al. 2007).

| Geometrical Data | Impeller | Diffuser |
|---|---|---|
| Inlet diameter, $d_i$ (mm) | 210.87 | 876 |
| Outlet diameter, $d_o$ (mm) | 796 | 1258 |
| Inlet span, $h_i$ (mm) | 103.91 | 43.8 |
| Outlet axial span, $h_o$ (mm) | 43.8 | 43.8 |
| Inlet blade angle, $\alpha_i$ (°) | 28 | 17 |
| Outlet blade angle, $\alpha_o$ (°) | 58 | 29 |
| Number of blades, n | 20 | 19 |

Simulation is conducted at 3000 RPM. The interface is located approximately midway between upstream trailing edges of the impeller and downstream leading edges of the diffuser.

The geometry of the compressor will be developed using AutoBlade software, a software for modeling the geometry of turbomachinery equipment by NUMECA. The resulting geometry is shown in **Figure 7**.
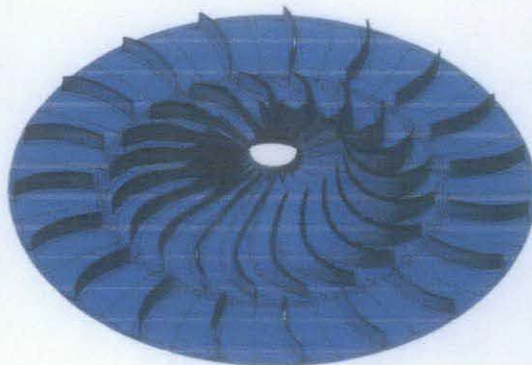


**Figure 7:** Geometry model of the centrifugal compressor.

# CHAPTER 4:

# RESULTS AND DISCUSSION

## 4.1 Results and Analysis from Test Variations

The test variations were performed to select the best alternative for running the simulation of the compressor. The meshing test is for finding the minimum meshing size required to get the best result, while the discretization test is to find the most suitable discretization for getting the best result. This is to minimize both cost and time consumption when running the simulation again later.

### 4.1.1 Test Variation 1: Meshing

Four meshing were produced for the first test variation, and the corresponding meshing is as shown in **Figure 8**.
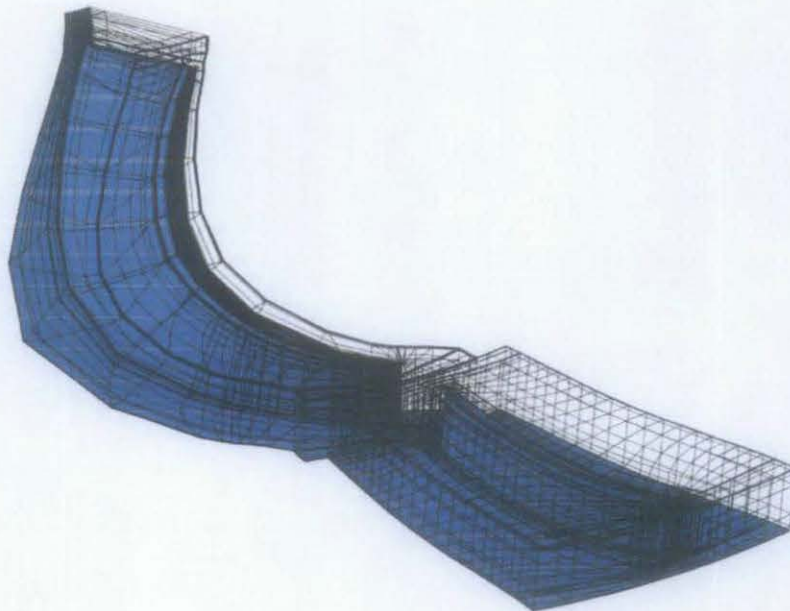


**Figure 8:** Initial meshing for the first test variation (310,567 grid points).

The results for meshing test variations are shown in **Table 4**.

**Table 4:** Results for meshing test variation.

| Test variation | M1_CEN_BL | M2_CEN_BL | M3_CEN_BL | M4_CEN_BL |
|---|---|---|---|---|
| Number of grid points | 310,567 | 767,023 | 2,274,698 | 2,771,123 |
| Inlet mass flow (kg/s) | 2.467 | 2.455 | 2.454 | 2.460 |
| Outlet mass flow (kg/s) | 2.457 | 2.461 | 2.459 | 2.462 |
| Mass flow error (%) | 0.412 | 0.234 | 0.213 | 0.058 |
| Efficiency | 0.5643 | 0.5990 | 0.6059 | 0.6073 |
| Pressure ratio | 1.080 | 1.084 | 1.085 | 1.085 |
| Axial thrust (N) | $5.817 \times 10^4$ | $5.834 \times 10^4$ | $5.835 \times 10^4$ | $5.852 \times 10^4$ |
| Torque (N·m) | -90.07 | -88.78 | -89.84 | -90.28 |

From the meshing test variation, the largest number of grid points was identified as the best (M4), due to having the lowest error for mass flow. However, all parameters can be considered comparable between each of the test variation in meshing.

### 4.1.2 Test Variation 2: Discretization

The discretization test variation was run by using M4 grid points, and the result for discretization test variations are as in **Table 5**.

**Table 5:** Result for discretization test variation.

| Test variation | M4_UPW1_BL | M4_TVD_BL | M4_FLUX_BL | M4_CEN_BL |
|---|---|---|---|---|
| Number of grid points | 2,771,123 | 2,771,123 | 2,771,123 | 2,771,123 |
| Inlet mass flow (kg/s) | 2.460 | 2.448 | 2.451 | 2.460 |
| Outlet mass flow (kg/s) | 2.460 | 2.447 | 2.444 | 2.462 |
| Mass flow error (%) | 0.017 | 0.035 | 0.307 | 0.058 |
| Efficiency | 0.4962 | 0.6306 | 0.6082 | 0.6073 |
| Pressure ratio | 1.075 | 1.090 | 1.090 | 1.085 |
| Axial thrust (N) | $5.847 \times 10^4$ | $5.844 \times 10^4$ | $5.851 \times 10^4$ | $5.852 \times 10^4$ |
| Torque (N·m) | -98.94 | -91.53 | -92.68 | -90.28 |

From discretization test variation, the $2^{nd}$ order central (CEN) was decided as the best discretization due to having a low mass flow error. Although the $1^{st}$ order upwind had the lowest mass flow error, its efficiency is significantly lower than the others. On the other hand, both the second order upwind discretization give lower values of mass flow rate as compared to the initial second order central.

### 4.1.3 Comparisons of Static Pressure Profile along the Cuts

For each test variation, three cuts are made and the corresponding static pressure profiles were plot according to its respective X. **Figure 9** shows the location of the cuts, while **Figure 10** and **Figure 11** shows the static pressure and axial velocity profiles along the three cuts.
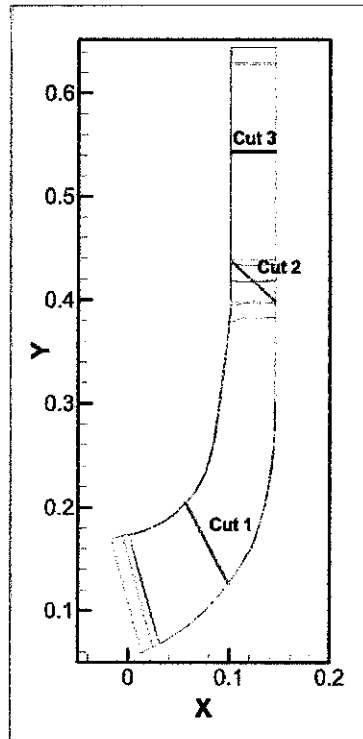


**Figure 9:** Location of the cuts.

It can be observed that from the figures of static pressure comparison that the M3 mesh does not give agreeable result with other plots. Thus, the test for M4 size needs to be carried out to see the trend, and since it is quite in agreement with the first two mesh sizes, M4 is considered as the best mesh size from the meshing test. However, M1 does not have enough points for solving the velocity profile at the intersection of impeller and diffuser smoothly.

For discretization test, it can be observed also that the upwind first order is the worst discretization, since some of the plots are very different from the others. This is true since the error for first order discretization is bigger compared to the higher order of discretization. For the second order upwind, both schemes give a comparable result with other test cases.
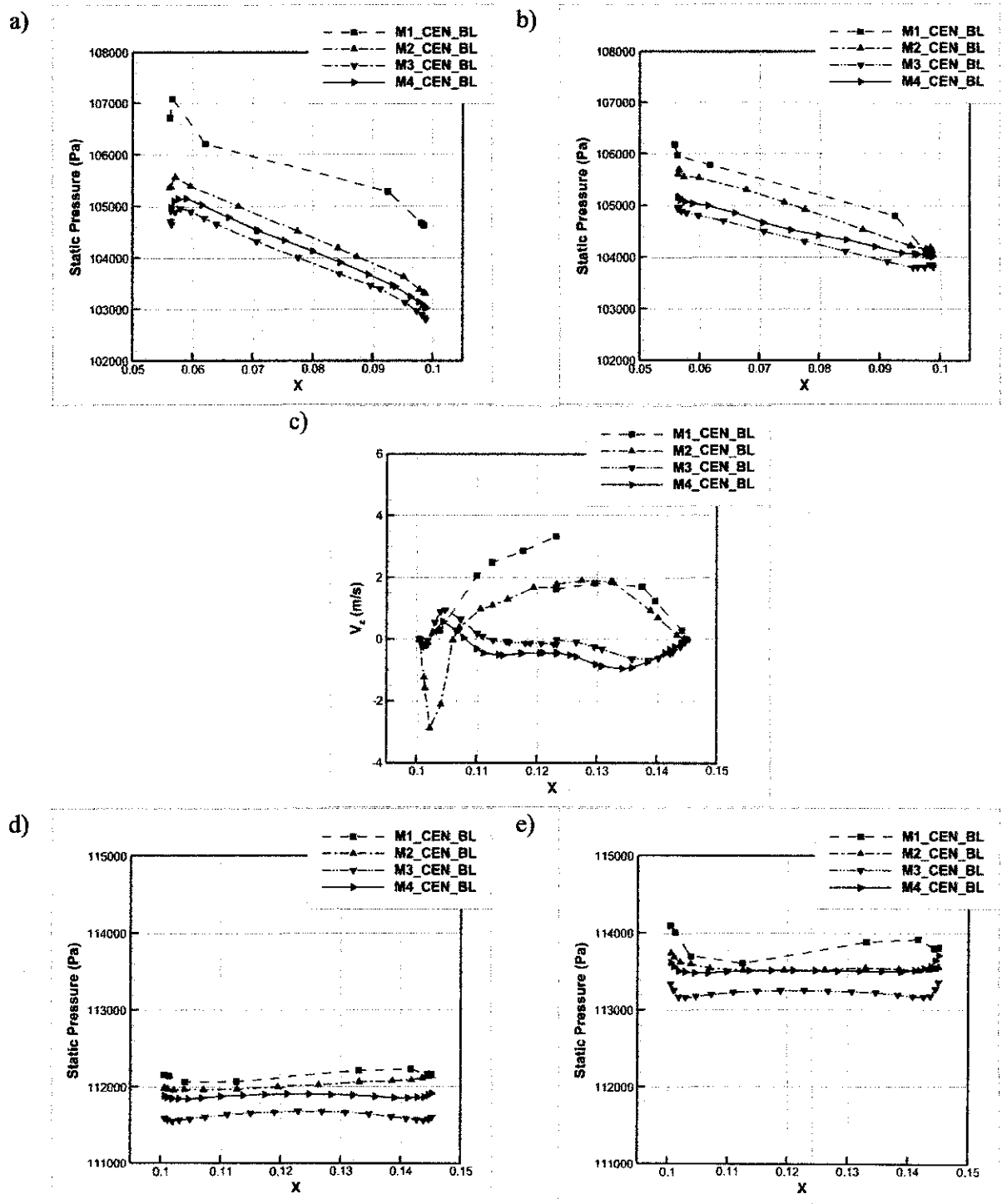
19

**Figure 10:** Comparison of NUMECA results among meshing test variations; (a) static pressure profile at the first cut, suction side; (b) static pressure profile at the first cut, pressure side; (c) axial velocity profile at the second cut; (d) static pressure profile at the third cut, suction side; and (e) static pressure profile at the first cut, pressure side.

20

**Figure 11:** Comparison of NUMECA results among discretization test variations; (a) static pressure profile at the first cut, suction side; (b) static pressure profile at the first cut, pressure side; (c) axial velocity profile at the second cut; (d) static pressure profile at the third cut, suction side; and (e) static pressure profile at the first cut, pressure side.
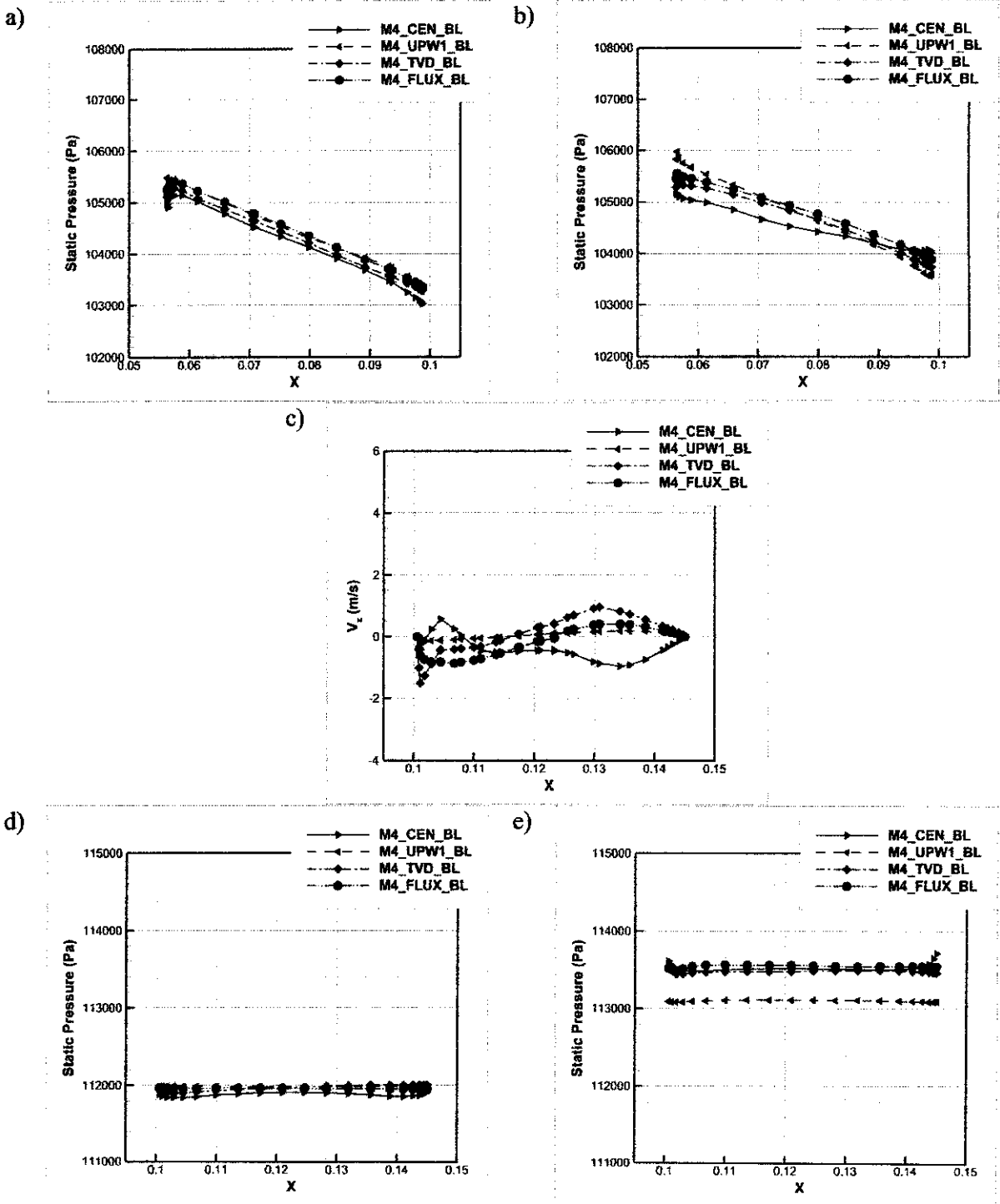
## 4.2 Comparison and Validation of the Best Alternative with the Published Journal Data

From the previous test variations, M4_BL_CEN was decided as the best alternative for the simulation. Therefore, the result of M4_BL_CEN will be compared with the result from journal (Zhou, Xi, & Cai, 2007). The comparisons are shown in **Figure 12** for axial velocity and **Figure 13** for static pressure.

Since there is no boundary conditions specified in the journal, the inlet boundary condition is taken to be the axial velocity, $V_z = 25$ m/s, and for the outlet, the static pressure is set at 113,000 Pa.
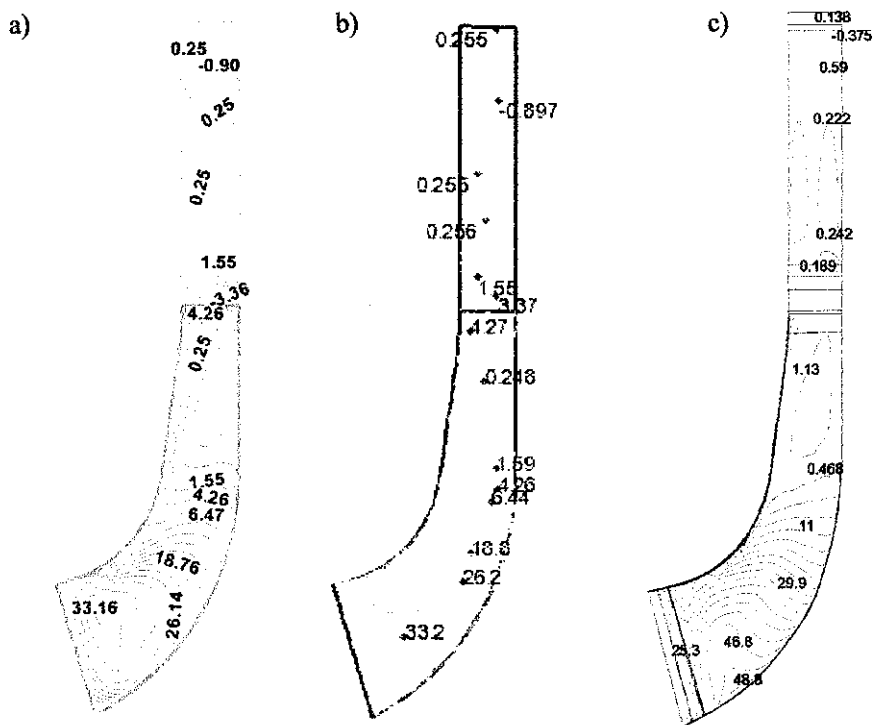


**Figure 12:** Comparison of axial velocity between (a) journal time-inclined operator, (b) journal NUMECA, and (c) M4_BL_CEN simulation.

22
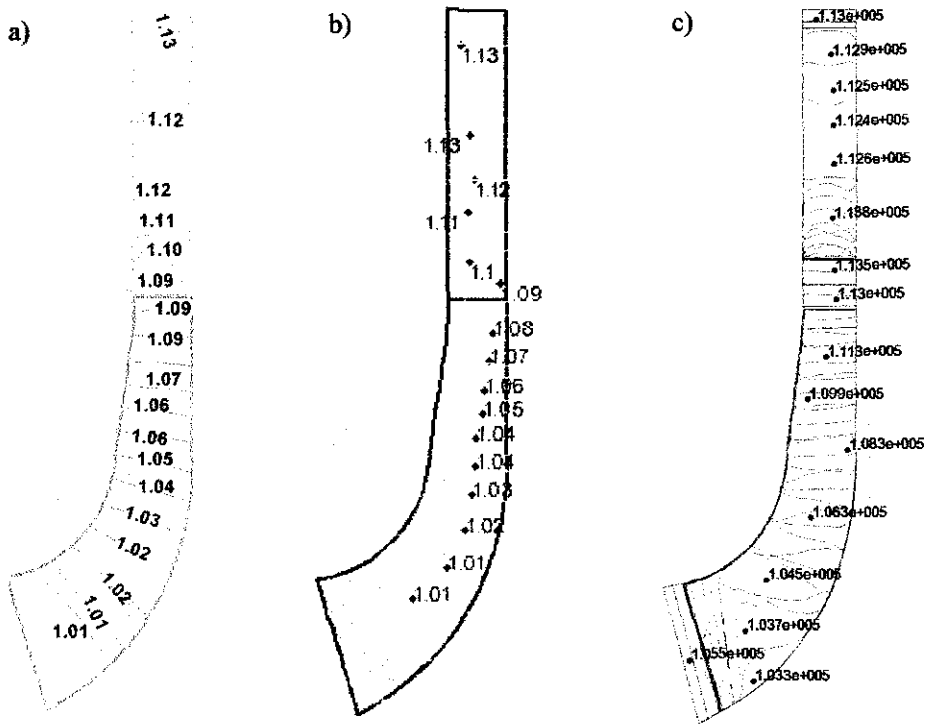
**Figure 13:** Comparison of static pressure between (a) journal time-inclined operator (in bar), (b) journal NUMECA (in bar), and (c) M4_BL_CEN simulation (in Pa).

It can be observed from the comparison that there are significant difference in the static pressure and axial velocity distribution. This may be due to the difference in the geometry of the compressor. However, for both simulation and journal, the highest value of axial velocity can be observed just after the leading edge of the impeller. There are also increment in static pressure along the diffuser section (but slightly in the simulation result), and negative velocity can be found near the outlet of the diffuser section.

## 4.3    Linking with HYSYS

The result of the simulation is then compared with value from HYSYS, to seek the agreement between values from both softwares. Values from NUMECA are being input into HYSYS (static temperature, static pressure, mass flow rate and efficiency) and the resulting static temperature at outlet is being compared with the static temperature from NUMECA.

**Table 6** shows the linking of values between HYSYS and NUMECA, with the resulting outlet temperature is being compared, and the difference is only 0.19%. This shows that the data can be linked between the two softwares with a good agreement. **Figure 14** shows the result of NUMECA simulation for static temperature and static pressure, in the azimuthal averaged solution.

**Table 6:** Linking values between HYSYS and NUMECA, with the resulting outlet static temperature is being compared.

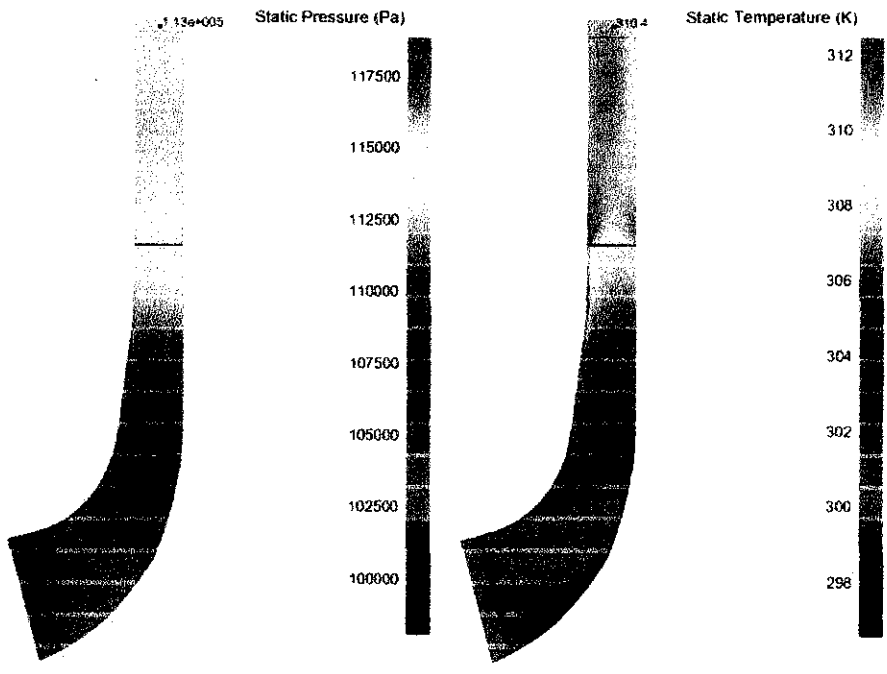| Parameters | | NUMECA | HYSYS |
|---|---|---|---|
| **Boundary conditions** | Inlet static pressure | 1.055 bar | |
| | Outlet static pressure | 1.13 bar | |
| | Inlet static temperature | 300 K | |
| **Obtained from NUMECA** | Efficiency | 0.6080 | |
| | Mass flow | 2.460 kg/s | |
| **To be compared** | Outlet static temperature | 310.4 K | 310.0 K |

**Figure 14:** Result of NUMECA simulation: Static pressure (in Pa, left) and static temperature (in K, right).

# CHAPTER 5:

# CONCLUSION AND RECOMMENDATION

## 5.1    Conclusion

A centrifugal compressor operation, which consists of 20 impeller blades and 19 diffuser blades, was successfully simulated using NUMECA FINE/Turbo. The geometry is done by using AutoBlade. The test variation were done next to find the best alternative for the simulation, with the meshing size of 2,771,213 grid points and second order central discretization were selected as the best condition to run the simulation, with Baldwin-Lomax turbulence model.

The result is then validated with Zhou et al. (2007), and despite some difference in result due to the difference in geometry of the compressor, some similarities can be observed between the two results such as the highest value of axial velocity can be observed just after the leading edge of the impeller, increment in static pressure along the diffuser section (but slightly in the simulation result), and negative velocity can be found near the outlet of the diffuser section.

The comparison of NUMECA data with HYSYS shows a small error of 0.19% for the outlet static temperature, and it can be concluded that the data between NUMECA and HYSYS can be linked with a good agreement.

## 5.2 Recommendation

For future research, the test variation can also include the turbulence model to see either there is a significant difference in results between different types of turbulence model.

The validation of the result, if possible, involves the experimental data from any published journals, or any turbomachinery equipments simulated, if available. This will ensure that the simulation result is in a higher degree of accuracy with real life condition.

The scope of the compressor geometry can also be widen to include the impeller with splitters, as well as with vaneless diffuser. It may be interesting to see the difference, if any, that may result from the different geometry. Plus, other type of turbomachinery equipments can also be included for study in the future.

# REFERENCES

Becker, B., Reyer, M., & Swoboda, M. (2007). Steady and unsteady numerical investigation of transitional shock-boundary-layer-interactions on a fan blade. *Aerospace Science and Technology, 11*, 507-517.

Celik, I. B. (1999). *Faculdade de Engenharia Mecanica.* Retrieved December 19, 2011, from Introductory Turbulence Modeling: http://www.fem.unicamp.br/~im450/palestras%26artigos/ASME_Tubulence/cds13workbook.pdf

Cengel, Y. A., & Boles, M. A. (2006). *Thermodynamics: An Engineering Approach* (5th ed.). McGraw-Hill Higher Education.

Derakhshan, S., Mohammadi, B., & Nourbakhsh, A. (2008). Incomplete sensitivities for 3D radial turbomachinery blade optimization. *Computers & Fluids, 37*, 1354-1363.

Dickmann, H. P., Wimmell, T. S., Szwedowicz, J., Filsinger, D., & Roduner, C. H. (2006). Unsteady flow in a turbocharger centrifugal compressor: Three-dimensional computational fluid dynamics simulation and numerical and experimental analysis of impeller blade vibration. *Journal of Turbomachinery, 128*(3), 455-465.

Fabrega, F. M., Rossi, J. S., & d'Angelo, J. V. (2010). Exergetic analysis of the refrigeration system in ethylene and propylene production process. *Energy, 35*(10), 1224-1231.

Konukman, A. E., & Akman, U. (2005). Flexibility and operability analysis of a HEN-integrated natural gas expander plant. *Chemical Engineering Science, 60*(24), 7057 – 7074.

Logan, J. E., Kadambi, V., & Roy, R. (2003). Introduction. In J. E. Logan, & R. Roy, *Handbook of Turbomachinery* (2nd ed., pp. 1-35). Marcel Dekker, Inc.

Marconcini, M., Rubechini, F., & Ibaraki, S. (2008). Numerical Investigation of a Transonic Centrifugal Compressor. *Journal of Turbomachinery, 130*, 1-9.

Missirlis, D., Yakinthos, K., Storm, P., & Goulas, A. (2007). Modeling pressure drop of inclined flow through a heat exchanger for aero-engine applications. *International Journal of Heat and Fluid Flow, 28*, 512-515.

Moran, M. J., & Shapiro, H. N. (2006). *Fundamentals of Engineering Thermodynamics* (5th ed.). John Wiley and Sons, Inc.

Peng, W. W. (2008). *Fundamentals of Turbomachinery.* John Wiley & Sons, Inc.

Ubaldi, M., Zunino, P., & Giglione, A. (1997). Detailed flow measurements within the impeller and the vaneless diffuser of a centrifugal turbomachine. *Experimental Thermal and Fluid Science, 17*, 147-155.

Zanganeh, K. E., Shafeen, A., & Salvador, C. (2009). CO2 Capture and Development of an Advanced Pilot-Scale Cryogenic Separation and Compression Unit. *Energy Procedia, 1*(1), 247-252.

Zhou, L., Xi, G., & Cai, Y. H. (2007). Unsteady numerical simulation in a centrifugal compressor using the time-inclined operator. *Journal of Aerospace Engineering, 221*(5), 795-804.